

## Electronic structure analysis for group III acceptors in Ge under stress considering screening effect and central-cell correction

This content has been downloaded from IOPscience. Please scroll down to see the full text.

2009 J. Phys.: Condens. Matter 21 335801

(<http://iopscience.iop.org/0953-8984/21/33/335801>)

View [the table of contents for this issue](#), or go to the [journal homepage](#) for more

Download details:

IP Address: 140.113.38.11

This content was downloaded on 25/04/2014 at 07:43

Please note that [terms and conditions apply](#).

# Electronic structure analysis for group III acceptors in Ge under stress considering screening effect and central-cell correction

T H Wang and S T Yen

Department of Electronics Engineering, National Chiao Tung University,  
1001 Ta-Hsueh Road, Hsinchu, Taiwan 30050, Republic of China

E-mail: [styen@cc.nctu.edu.tw](mailto:styen@cc.nctu.edu.tw)

Received 6 April 2009, in final form 6 July 2009

Published 24 July 2009

Online at [stacks.iop.org/JPhysCM/21/335801](http://stacks.iop.org/JPhysCM/21/335801)

## Abstract

We study theoretically the electronic structures of various group III acceptors in Ge under [001] stress, based on the effective-mass theory with a semi-empirical impurity potential which considers the  $q$ -dependent screening and the central-cell correction. An assignment is made for inter-level transition lines which were previously ignored or incorrectly assigned. In addition, our calculation can resolve crowding levels of final states of transition lines which have not been resolved by experimental techniques. The stress effect on the electronic structure can be understood by connecting with the composition of the states. Our results show that the binding energies decrease rapidly with the stress in the low-stress region, and for even-parity states they exhibit remarkable asymmetry in the stress dependence due to the large difference between the heavy-hole and the light-hole compositions. The acceptor states asymptotically approach a pure heavy-hole or light-hole state under high stress. In the limiting case of high stress, extra degeneracy appears. The central-cell correction may cause a significant chemical shift for even-parity states of nonisocoric acceptors. We also complete the assignment of the four line components into which the  $B$  line splits under stress. The newly assigned stress-dependent transition energies show excellent agreement with the experimental data for low stress. A justification is made for the applicability of our calculation scheme to the case of high stress.

(Some figures in this article are in colour only in the electronic version)

## 1. Introduction

The problem of impurity levels in semiconductors has been extensively studied. Reliable experimental spectra of group III acceptors in Ge have been available for more than three decades [1–4]. Even though it has been over half a century since the effective-mass approximation (EMA) of Luttinger and Kohn [5], the applicability of the EMA to the impurity problem is still an open issue and modification within the framework of the EMA is under development. Pantelides and Sah [6, 7] evaluated the EMA by calculating the energy levels of donors in Si with first-principles impurity potentials. They found the EMA is not only applicable to shallow levels but also to deep levels for isocoric impurities, and the applicability can be extended to the case of nonisocoric impurities just by adding a reorthogonalization term to the impurity potential

of [6], according to the general theory of pseudopotentials [8]. Baldereschi and Lipari [9, 10] calculated the energy levels of group III acceptors in Ge, giving results in a quantitative agreement with experiment. Their studies not only justify the applicability of the EMA to the group III acceptors in Ge but also demonstrate the importance of the  $q$ -dependent dielectric screening and the components of high angular momenta (up to  $l = 7$ ) of the acceptor states. Lipari *et al* [11] calculated the even-parity states of various species of group III acceptors in Ge and in Si by introducing into a semi-empirical impurity potential a short-range part of a simple local form including the central-cell correction. In addition, Buczko and Bassani [12] performed a similar study by using an impurity potential of a different form and yielded results also consistent with experiment. These studies provide the foundation for using the semi-empirical potential with the central-cell effect in the

impurity level calculation [11, 12]. Recently, because of the advent of strained p-Ge terahertz lasers [13], the stress effect on acceptor states in Ge has drawn much attention. Several studies have been done regarding the stress effect on the acceptor levels [14–16]. However, there has been no study on the acceptor states considering simultaneously the  $q$ -dependent dielectric screening, the central-cell correction and the stress effect.

In this paper, we calculate the electronic structure, mainly focused on the stress effect along the [001] direction, of various group III acceptors in Ge by the EMA with a simple semi-empirical potential including the  $q$ -dependent dielectric screening and the central-cell correction. The stress effect on the impurity levels is analyzed by inspecting the heavy-hole (HH) and the light-hole (LH) compositions of the states. Our results give excellent agreement with experiments both for zero stress [1–4] and for stress up to 0.35 kbar [17, 18], confirming the importance of the central-cell correction in the energy levels of nonisocoric acceptors. This allows us to complete the identification of the inter-level absorption lines, some of which were previously ignored or incorrectly assigned. Importantly, we make a systematic assignment for the transition lines of [19] associated with an even-parity state as the final state. The stress we consider in the study extends to 10 kbar, but there have been no experimental data at high stress for comparison. Therefore, we make a discussion on the validity of our calculation scheme in the case of high stress.

This paper is organized as follows. We first present the theoretical approaches in section 2. It is then followed by the principal part of the paper in section 3 which shows the calculated impurity levels, line assignment, the stress effect, the extra degeneracy, the chemical shifts and the applicability of the semi-empirical potential for the impurity to the case of high stress. Finally, we draw conclusions in section 4.

## 2. Theoretical approaches

The acceptor states in strained Ge are treated with the six-band effective-mass Hamiltonian [5] modified by the Bir–Pikus deformation theory [20]. Such a model expresses explicitly the coupling of the HH, the LH and the spin–orbit split-off hole (SO) bands, and also implicitly includes the coupling from remote bands. In the coordinate system transformed in compliance with the deformation, the wavefunctions of the acceptor states are written as

$$\Psi = \sum_{v=1}^6 F_v \Phi_{M_v}^{J_v}, \quad (1)$$

where  $\Phi_{M_v}^{J_v}$  are the Bloch functions at the  $\Gamma$  point of bands  $v$  ( $v = 1, 2, \dots, 6$ ) in the Brillouin zone, which transform in the  $\bar{T}_d$  group like atomic functions having angular momentum quantum number  $J_v$  and magnetic quantum number  $M_v$ . Four of them are the basis functions of the  $\Gamma_8^+$  representation ( $J_v = 3/2$ ) in the  $\bar{O}_h$  group and the other two are those of the  $\Gamma_7^+$  representation ( $J_v = 1/2$ ). The  $F_v$  are the envelope functions

which are the solutions of the effective-mass equation:

$$\sum_{v=1}^6 H_{\mu v} F_v = E F_{\mu}, \quad \mu = 1, 2, \dots, 6. \quad (2)$$

The  $E$  is the energy of the acceptor state. The  $H_{\mu v}$  are the elements of the effective-mass Hamiltonian which can be written as

$$H = H_0 + V(r)I, \quad (3)$$

where  $H_0$  is the  $6 \times 6$  unperturbed Hamiltonian considering the coupling caused only by the  $\mathbf{k} \cdot \mathbf{p}$  perturbation and the strain, if present, for the perfect host crystal. The detailed form of  $H_0$  can be found in the literature [16, 21]. In the general case, three deformation potentials,  $a$ ,  $b$  and  $d$ , are required in  $H_0$  to describe the strain-induced changes in the electronic energies of valence bands [16]. For the uniaxial stress along the [001] direction, we need only  $b$  in the calculation if we neglect the hydrostatic strain which just shifts the valence bands as a whole. The parameter  $b$  is the proportionality constant for the relative splitting between the HH and the LH band edges caused by strain; it gives an energy splitting of  $2b(\varepsilon_{zz} - \varepsilon_{xx})$ , where  $\varepsilon_{zz}$  and  $\varepsilon_{xx}$  are the normal strains along [001] and [100], respectively [20]. In the second term of equation (3),  $I$  is the  $6 \times 6$  unit matrix and  $V(r)$  is the impurity potential for which we adopt in this study the semi-empirical form:

$$V = V_C + V_{cc}, \quad V_C = -\frac{2}{r}[1 + (\epsilon - 1)e^{-\alpha r}], \quad (4)$$

$$V_{cc} = \frac{A}{r}e^{-\beta r},$$

where  $\epsilon$  is the dielectric constant, and  $\alpha$ ,  $\beta$  and  $A$  are parameters. In the expressions we use dimensionless units. The length and the energy are in effective Bohr radius  $a\epsilon\gamma_1$  and effective Rydberg  $R/\epsilon^2\gamma_1$ , respectively, where  $a$ ,  $R$  and  $\gamma_1$  are the Bohr radius, the Rydberg energy and the first Luttinger parameter, respectively. The impurity potential  $V$  is a consequence of the difference between the Hamiltonians with and without the host atom replaced by the acceptor atom in the crystal. It can be considered as composed of two parts. The first part is the Coulomb contribution  $V_C$  caused directly by the negative point charge of the acceptor ion modified by the  $q$ -dependent dielectric screening [11]. The remaining part, called the central-cell correction  $V_{cc}$ , accounts for all the difference  $H - H_0$  but the screened Coulomb potential of the point charge. It primarily includes the difference in an effective ‘attractive’ force which the atomic core states exert on the hole of interest, as well as the effect of the lattice relaxation around the impurity site induced by the presence of the impurity [12, 22]. Such an effective force, corresponding to the kinetic energy of the valence electron, originates from the orthogonality of the valence state to the core states. From the standpoint of a hole, the force is attractive. As a result, the central-cell correction  $V_{cc}$  is short-range in nature and, strictly speaking, has a tetrahedral symmetry in the absence of external stress. In the study, we suppose  $V_{cc}$ , for simplicity, to have a simple form which is spherically symmetric and neglects the nonlocality effect. It is thus expected that the  $V_{cc}$  is small for

the isocoric acceptor Ga, positive for B and Al, and negative for In and Tl because the heavier ions exert a stronger effective attractive force on the hole.

To solve the effective-mass equation (2), we expand the envelope functions in a sum of products of radial functions and spherical harmonics:

$$F_v = \sum_{lm} f_v^{lm}(r) Y_{lm}(\theta, \phi). \quad (5)$$

Symmetry considerations can save much labor in the calculation. For the acceptor center substitutively placed at an atomic site in Ge under a stress along the [001] direction, the Hamiltonian has a tetragonal symmetry with the transformation elements forming the  $D_{2d}$  group. For double group  $\bar{D}_{2d}$ , there are only two irreducible representations  $\Gamma_6$  and  $\Gamma_7$ , both of which have a dimension of 2. Therefore, the acceptor states are always twofold-degenerate, except for accidental degeneracy, and can transform according to either  $\Gamma_6$  or  $\Gamma_7$ . Moreover, in spite of the lack of inversion symmetry of the problem, the envelope functions of an acceptor state can all have a common parity since the effective-mass Hamiltonian is invariant under inversion about the impurity site. Therefore, acceptor states can be classified to  $\Gamma_6^+$ ,  $\Gamma_6^-$ ,  $\Gamma_7^+$  or  $\Gamma_7^-$ , where the superscripts denote the parity of the envelope functions. It follows that the sum in (5) requires running only over the terms which have the same parity. Furthermore, we need only to work out one of the basis-function doublets for each irreducible representation by the present calculation scheme. The other one can be obtained simply by the time-reversal operation. In conformity with the transformation properties, the values of  $m$  in (5) for the basis-function doublet to be dealt with are under the restriction

$$m = \begin{cases} 4n + \frac{3}{2} - M_v & \text{for } \Gamma_6^+ \\ 4n + \frac{1}{2} - M_v & \text{for } \Gamma_7^+ \\ 4n - \frac{1}{2} - M_v & \text{for } \Gamma_6^- \\ 4n - \frac{3}{2} - M_v & \text{for } \Gamma_7^-, \end{cases} \quad (6)$$

where  $n$  is an integer. Such a choice of the angular parts for the envelope functions is equivalent to the one of Buczko [16], although different in formulation.

The problem now becomes the one of solving the radial parts of the envelope functions. We expand them in the following form [12]:

$$f_v^{lm}(r) = r^L \sum_i c_{vi}^{lm} e^{-\alpha_i r}, \quad (7)$$

to conform with a set of coupled equations of the radial parts, where the numbers  $\alpha_i$  in the exponents are chosen to form a geometric progression. The value of  $L$  is chosen, depending on  $l$ , according to the following rule:

$$L = \begin{cases} 0 & \text{for } l = 0 \\ 1 & \text{for } l = 1 \text{ and any positive even number} \\ 2 & \text{for } l = \text{any odd number other than 1.} \end{cases}$$

**Table 1.** Some material parameters of the host crystal Ge used in the calculation. The  $\gamma_1$ ,  $\gamma_2$  and  $\gamma_3$  are Luttinger's parameters,  $\Delta$  the spin-orbit splitting,  $C_{11}$  and  $C_{12}$  the stiffness constant, and  $b$  the deformation potential.

Parameter	Ge
$\gamma_1$ [23]	13.38
$\gamma_2$ [23]	4.24
$\gamma_3$ [23]	5.69
$\Delta$ [24]	296 (meV)
$C_{11}$ [25]	1240 (kbar cm <sup>-2</sup> )
$C_{12}$ [25]	413 (kbar cm <sup>-2</sup> )
$b$	-2.63 (eV)

### 3. Results and discussion

In the calculation, we take the values reported in table 1 for the host crystal parameters to be used in the effective-mass theory. Here, the value of the deformation potential  $b = -2.63$  eV is determined by a best fit to the experimental stress dependence of the transition energy between  $1\Gamma_6^+$  and  $1\Gamma_7^+$  of [18]. (Here, as in [11], the number  $n$  in  $n\Gamma_i^u$  ( $i = 6, 7, 8; u = +, -$ ) is used to denote the order of the states with symmetry  $\Gamma_i^u$  according to the order of their energies from low to high.) The dielectric constant  $\epsilon$  and the parameter  $\alpha$  for the acceptor Coulomb potential are set at 15.36 and  $0.93\epsilon\gamma_1$ , respectively, as in the work of [11] and [26]. For the central-cell potential,  $\beta$  is set at  $1.00\epsilon\gamma_1$  and  $A$  is an adjustable parameter, as in the work of [22]. By fitting the calculated to the experimental values of the  $D$  line transition energy for various species of acceptors in Ge [1–3], we determine the  $A$  values to be 28.96, 7.52, 1.00, -13.71 and -26.29 for B, Al, Ga, In and Tl, respectively, in agreement with the previous argument about the central-cell potential.

#### 3.1. Line assignment for acceptors in unstrained Ge

Listed in table 2 are the calculated transition energies for the hole from the lowest odd-parity state  $1\Gamma_8^-$  to the higher even-parity states of unstrained Ge:B together with the experimental data of [19] for comparison. Lipari *et al* [11] and Kurskii [27] have identified a single level of  $2\Gamma_8^+$  for Ge:B by assigning the  $E$  line in [1] to the transition from  $1\Gamma_8^+$  to  $2\Gamma_8^+$ . Here, we identify systematically the levels of even-parity states  $\Gamma_i^+$  ( $i = 6, 7, 8$ ) by assigning the lines of transitions in [19], as table 2 shows. The assignment is found to be excellent. Also, our calculation can give additional energy levels of even-parity states which have not been resolved yet by experiment. Gershenzon *et al* [19] associated the lines at 2.435 and 2.485 meV with the  $G^* \rightarrow C^*$  transition where the symbol  $G^*$  corresponds to the  $1\Gamma_8^-$  level and the  $C^*$  corresponds to the set of the  $3\Gamma_8^+$ ,  $1\Gamma_7^-$  and  $3\Gamma_8^-$  levels. Excluding the  $1\Gamma_8^- \rightarrow 1\Gamma_7^-$  and the  $1\Gamma_8^- \rightarrow 3\Gamma_8^-$  transitions, which are almost electric-dipole-forbidden, we assign the line at 2.435 meV to the  $1\Gamma_8^- \rightarrow 3\Gamma_8^+$  transition while the line at 2.485 meV is assigned to the  $2\Gamma_8^+ \rightarrow 3\Gamma_6^-$  transition whose energy is 2.481 meV in our calculation.

For completeness, we also make assignments for the lines associated with transitions from the ground state  $1\Gamma_8^+$  to the

**Table 2.** The transition energies from the  $1\Gamma_8^-$  state to the higher even-parity states of unstrained Ge:B. The experimental data are taken from [19] and the number in parentheses attached to each of the data is the sample number.

Final state	Transition energy from $1\Gamma_8^-$ (meV)	
	Present work	Experimental data
$2\Gamma_8^+$	1.36	1.365 (23)
$3\Gamma_8^+$	2.43	2.435 (44)
$1\Gamma_6^+$	2.85	2.865 (48)
$4\Gamma_8^+$	2.92	2.91 (49)
$1\Gamma_7^+$	3.25	3.26 (51)
$5\Gamma_8^+$	3.30	3.3 (52)
$6\Gamma_8^+$	3.36	3.37 (53)
$2\Gamma_6^+$	3.47	3.48 (54)
$7\Gamma_8^+$	3.55	
$3\Gamma_6^+$	3.58	3.585 (55)
$2\Gamma_7^+$	3.75	
$8\Gamma_8^+$	3.76	
$9\Gamma_8^+$	3.79	3.79 (56)
$10\Gamma_8^+$	3.84	
$4\Gamma_6^+$	3.87	
$11\Gamma_8^+$	3.88	3.875 (57)
$3\Gamma_7^+$	3.88	
$12\Gamma_8^+$	3.90	3.89 (58)
$5\Gamma_6^+$	3.92	3.925 (59)

odd-parity states. The calculated transition energies for various species of acceptors in unstrained Ge are listed in table 3, together with experimental data of transition lines currently accessible. As can be seen, our calculation not only results in excellent assignments but also resolves crowding levels of final states for observed single transitions which have not been resolved by experiment. For instance, the  $C$  line is associated with the transition lines  $1\Gamma_8^+ \rightarrow (1\Gamma_7^-, 3\Gamma_8^-)$  and the  $A_3$  line associated with the transitions  $1\Gamma_8^+ \rightarrow (2\Gamma_7^-, 1\Gamma_6^-, 6\Gamma_8^-)$ .

### 3.2. Stress effect on acceptor electronic structure

Now that the parameters we take have led to satisfactory accuracy in acceptor levels of unstrained Ge, we take them further to calculate the acceptor levels of Ge under stress. Figures 1 and 2 show the binding energies of even- and odd-parity states, respectively, for Ge:Ga as functions of uniaxial stress along the [001] direction. The panels (b) of the two figures are enlargements of panels (a) so that the curves of several excited states of low binding energy are distinguishable. A positive (negative) stress means a compressive (tensile) stress. The binding energy of an acceptor state is the minimum energy required to liberate a hole bound at the state, that is, the difference in energy between the state and the nearest valence band edge. Since the valence band edges vary with the stress, we calculate and plot the edges of the HH, the LH and the SO bands as functions of [001] stress in figure 3 for convenience in later analysis. With the compressive stress, the LH (HH) band edge moves monotonically upwards (downwards), while with tensile stress the HH (LH) band edge moves upwards (downwards). Accordingly, we have  $E_B(n\Gamma_i^u) = E(n\Gamma_i^u) - E_{LH}$  for compressive stress and  $E_B(n\Gamma_i^u) = E(n\Gamma_i^u) - E_{HH}$  for tensile stress, where  $E_B(n\Gamma_i^u)$

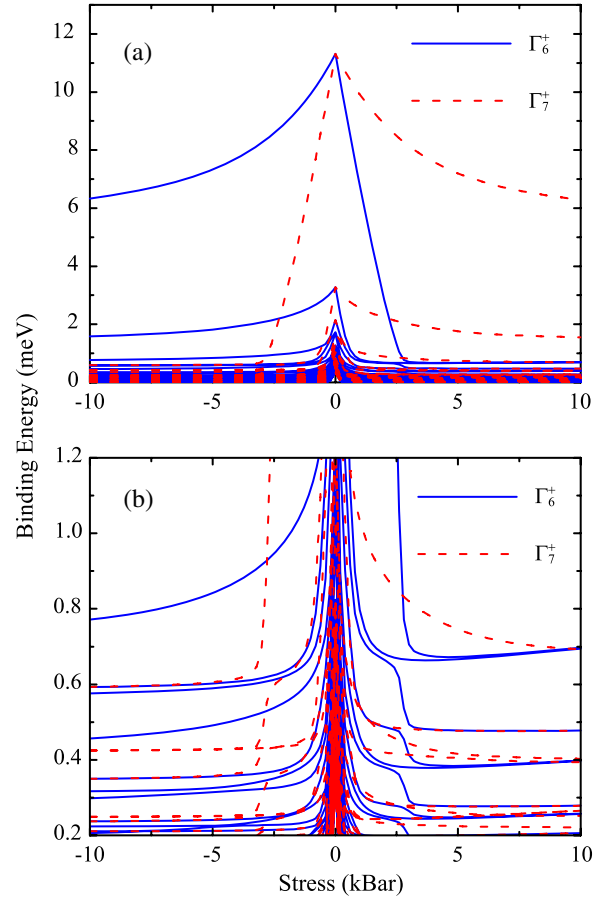


**Figure 1.** Binding energies of even-parity states as functions of uniaxial stress along the [001] direction for Ge:Ga. The positive (negative) stress means a compressive (tensile) stress. Panel (b) is an enlargement of panel (a).

and  $E(n\Gamma_i^u)$  are the binding energy and the energy level, respectively, of the  $n\Gamma_i^u$  state, and  $E_{LH}$  and  $E_{HH}$  are the LH and the HH band edges, respectively.

From figures 1 and 2, we find that the binding energies are susceptible to the stress in the region of low stress ( $<3$  kbar) but become more insensitive as the stress is large ( $>3$  kbar). Such stress dependence is related to the composition of the acceptor states. In the low-stress region, the states are composed in a manner that the HH composition ( $f_{HH}$ ) and the LH composition ( $f_{LH}$ ) are both significant but the SO composition is negligible since  $E(n\Gamma_i^u) - E_{HH} \approx E(n\Gamma_i^u) - E_{LH} \ll E(n\Gamma_i^u) - E_{SO}$ , where  $E_{SO}$  is the edge of the SO band. As compression increases, some higher-energy levels move downwards with the HH band and finally become resonant in nature after merging into the LH band. The other levels which remain above the LH band do not move with the HH band. As a result, the ratio  $f_{HH}/f_{LH}$  decreases with compression for the bound states because of the increase of  $E(n\Gamma_i^u) - E_{HH}$ . As the stress is sufficiently large such that  $E(n\Gamma_i^u) - E_{HH} \gg E(n\Gamma_i^u) - E_{LH}$ , the bound states are almost of LH character ( $f_{LH} \approx 1$  and  $f_{HH} \approx 0$ ). In the light of the variational principle, more basis functions are preferred at low stress to form the eigenfunctions of acceptor states than at high stress.

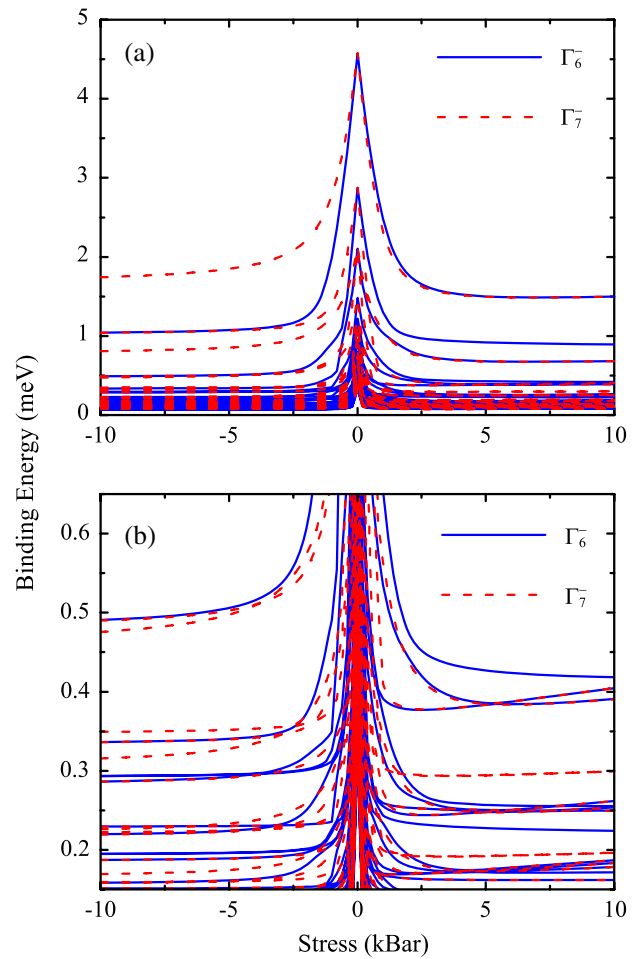
**Table 3.** The transition energies from the ground state  $1\Gamma_8^+$  to the odd-parity states for various group III acceptors in unstrained Ge. The symbols for transition lines given in the first column are defined as in [3].

Line	Final state	Transition energy from $1\Gamma_8^+$ (meV)									
		B		Al		Ga		In		Tl	
<i>G</i>	$1\Gamma_8^-$	6.233 <sup>a</sup>	6.21 <sup>b</sup>	6.569 <sup>a</sup>	6.59 <sup>c</sup>	6.734 <sup>a</sup>	6.72 <sup>d</sup>	7.376 <sup>a</sup>		8.848 <sup>a</sup>	8.91 <sup>b</sup>
<i>D</i>	$2\Gamma_8^-$	6.24 <sup>c</sup>	6.215 <sup>d</sup>	6.565 <sup>d</sup>	6.581 <sup>e</sup>	6.74 <sup>c</sup>		7.39 <sup>c</sup>		8.87 <sup>c</sup>	
		7.936 <sup>a</sup>	7.936 <sup>b</sup>	8.272 <sup>a</sup>	8.27 <sup>c</sup>	8.437 <sup>a</sup>	8.437 <sup>d</sup>	9.080 <sup>a</sup>	9.113 <sup>d</sup>	10.551 <sup>a</sup>	10.552 <sup>b</sup>
<i>C</i>	$1\Gamma_7^-$	7.94 <sup>c</sup>	7.936 <sup>d</sup>	8.272 <sup>d</sup>	8.28 <sup>e</sup>	8.44 <sup>c</sup>	8.441 <sup>e</sup>	9.08 <sup>c</sup>		10.57 <sup>c</sup>	
		8.685 <sup>a</sup>	8.681 <sup>b</sup>	9.021 <sup>a</sup>	9.02 <sup>c</sup>	9.186 <sup>a</sup>	9.185 <sup>d</sup>	9.829 <sup>a</sup>	9.864 <sup>d</sup>	11.301 <sup>a</sup>	11.3 <sup>b</sup>
<i>B</i>	$3\Gamma_8^-$	8.69 <sup>c</sup>	8.686 <sup>d</sup>	9.025 <sup>d</sup>	9.031 <sup>e</sup>	9.19 <sup>c</sup>	9.192 <sup>e</sup>	9.86 <sup>c</sup>		11.32 <sup>c</sup>	
		8.707 <sup>a</sup>		9.043 <sup>a</sup>		9.208 <sup>a</sup>		9.851 <sup>a</sup>		11.322 <sup>a</sup>	
<i>B</i>	$4\Gamma_8^-$	9.329 <sup>a</sup>	9.33 <sup>b</sup>	9.666 <sup>a</sup>	9.67 <sup>c</sup>	9.831 <sup>a</sup>	9.814 <sup>d</sup>	10.473 <sup>a</sup>	10.506 <sup>d</sup>	11.945 <sup>a</sup>	11.93 <sup>b</sup>
		9.32 <sup>c</sup>	9.32 <sup>d</sup>	9.654 <sup>d</sup>	9.665 <sup>e</sup>	9.84 <sup>c</sup>	9.825 <sup>e</sup>	10.48 <sup>c</sup>		11.92 <sup>c</sup>	
<i>A</i> <sub>4</sub>	$5\Gamma_8^-$	9.593 <sup>a</sup>		9.929 <sup>a</sup>	9.925 <sup>c</sup>	10.094 <sup>a</sup>		10.736 <sup>a</sup>		12.208 <sup>a</sup>	
		9.568 <sup>d</sup>		9.927 <sup>d</sup>		10.091 <sup>d</sup>		10.746 <sup>d</sup>			
<i>A</i> <sub>3</sub>	$2\Gamma_7^-$	9.665 <sup>a</sup>	9.66 <sup>b</sup>	10.002 <sup>a</sup>	10.02 <sup>c</sup>	10.167 <sup>a</sup>	10.152 <sup>d</sup>	10.809 <sup>a</sup>	10.828 <sup>d</sup>	12.281 <sup>a</sup>	12.29 <sup>b</sup>
		9.65 <sup>c</sup>	9.665 <sup>d</sup>	9.995 <sup>d</sup>	10.001 <sup>e</sup>	10.17 <sup>c</sup>		10.81 <sup>c</sup>		12.26 <sup>c</sup>	
<i>A</i> <sub>2</sub>	$1\Gamma_6^-$	9.669 <sup>a</sup>		10.005 <sup>a</sup>		10.170 <sup>a</sup>		10.813 <sup>a</sup>		12.285 <sup>a</sup>	
		9.682 <sup>a</sup>		10.018 <sup>a</sup>		10.183 <sup>a</sup>		10.826 <sup>a</sup>		12.297 <sup>a</sup>	
		9.798 <sup>a</sup>	9.79 <sup>b</sup>	10.134 <sup>a</sup>	10.15 <sup>c</sup>	10.299 <sup>a</sup>	10.287 <sup>d</sup>	10.942 <sup>a</sup>	10.955 <sup>d</sup>	12.413 <sup>a</sup>	12.42 <sup>b</sup>
<i>A</i> <sub>1</sub>	$3\Gamma_7^-$	9.81 <sup>c</sup>	9.785 <sup>d</sup>	10.13 <sup>d</sup>	10.113 <sup>e</sup>	10.31 <sup>c</sup>		10.96 <sup>c</sup>		12.43 <sup>c</sup>	
		9.879 <sup>a</sup>	9.863 <sup>d</sup>	10.215 <sup>a</sup>	10.198 <sup>d</sup>	10.380 <sup>a</sup>	10.36 <sup>d</sup>	11.023 <sup>a</sup>	11.033 <sup>d</sup>	12.494 <sup>a</sup>	

<sup>a</sup> Present work; <sup>b</sup> reference [2]; <sup>c</sup> reference [1]; <sup>d</sup> reference [3]; <sup>e</sup> reference [4].

This explains the facts that the binding energy is largest at zero stress and decreases rapidly with low stress but changes slowly with high stress. The situation of tensile stress is similar to that of compression, but with the roles of HH and LH replacing each other. Analogously, under a sufficiently high tensile stress, the acceptor states are almost of HH character. An exception occurs in the high-stress region where the binding energy slightly increases with compressive stress but slightly decreases with tensile stress. This is because at a high stress the HH–LH coupling in the acceptor states becomes unimportant and the effective mass is the dominant factor in the stress dependence of binding energy. The LH mass is increased by compressive stress but the HH mass is reduced by tensile stress.

There is a substantial difference in stress dependence of binding energy between the low-energy even-parity states and the low-energy odd-parity states in the low-stress region. From figure 1, it is seen that the binding energy of the  $1\Gamma_6^+$  ( $1\Gamma_7^+$ ) state decreases much more rapidly with the compressive (tensile) stress than with the tensile (compressive) stress. Such asymmetry does not appear so remarkably for the odd-parity states, as can be seen from figure 2. To realize the difference, it is instructive to invoke the correlation between the HH–LH coupling and the binding energy of an acceptor state. Figure 4 shows the HH composition  $f_{\text{HH}}$  and the LH composition  $f_{\text{LH}}$  of Ge:Ga acceptor states  $1\Gamma_6^+$  in (a),  $1\Gamma_7^+$  in (b),  $1\Gamma_6^-$  in (c) and  $1\Gamma_7^-$  in (d) as functions of [001] stress. The SO composition is negligibly small (less than 0.3%) and hence not shown here. We find from figure 4(a) that  $f_{\text{HH}} = 75\%$  and  $f_{\text{LH}} = 25\%$  for the  $1\Gamma_6^+$  state at zero stress, indicating that the  $1\Gamma_6^+$  state is like HH more than like LH in character. The compositions of the  $1\Gamma_6^+$  state change rapidly with the compressive stress but much more slowly with the tensile stress in the low-stress region. At a compressive stress above 3 kbar, the  $1\Gamma_6^+$  state becomes almost of LH character ( $f_{\text{HH}} \approx 0$  and  $f_{\text{LH}} \approx 100\%$ ) while for tensile stress it remains HH-like. At a tensile stress of

**Figure 2.** Binding energies of odd-parity states as functions of uniaxial stress along the [001] direction for Ge:Ga. The positive (negative) stress means a compressive (tensile) stress. Panel (b) is an enlargement of panel (a).

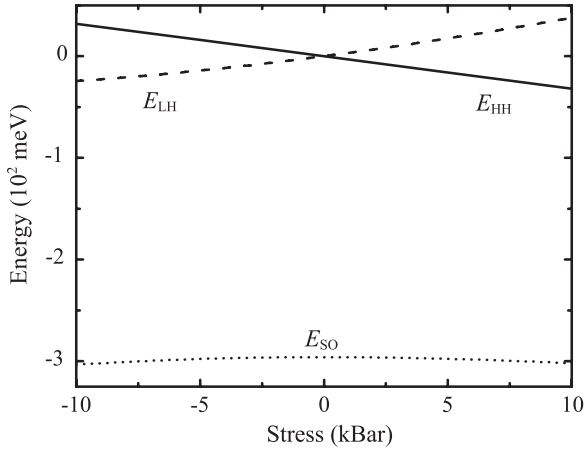


**Figure 3.** The HH, LH and SO band edges (denoted by  $E_{HH}$ ,  $E_{LH}$  and  $E_{SO}$ , respectively) as functions of uniaxial stress along the [001] direction for Ge:Ga. The positive (negative) stress means a compressive (tensile) stress.

3 kbar, the  $1\Gamma_6^+$  state does not become a purely HH-like state, but still contains an LH composition of about 10%. Such a rapid change in composition is the cause of the rapid reduction in binding energy with the compressive stress. For the  $1\Gamma_7^+$  state, the situation is reversed. As seen from figure 4(b), the  $1\Gamma_7^+$  state is LH-like with  $f_{LH} = 75\%$  at zero stress. It turns out to become almost purely HH-like after a rapid change in composition with the tensile stress, but remains still LH-like as its  $f_{LH}$  value increases slowly with the compressive stress. For the  $1\Gamma_6^-$  ( $1\Gamma_7^-$ ) state, as shown in figures 4(c) and (d),  $f_{LH} = 55\% > f_{HH}$  ( $f_{HH} = 55\% > f_{LH}$ ) at zero stress. This causes the binding energy of the  $1\Gamma_6^-$  ( $1\Gamma_7^-$ ) state to decrease with the tensile (compressive) stress more rapidly than with the compressive (tensile) stress, as figure 2 shows. The asymmetry in the stress dependence for the odd-parity states is not as prominent as for the even-parity states due to the small difference between  $f_{LH}$  and  $f_{HH}$  at zero stress.

In passing, we have known that the stress can shift the energy levels and also change the composition of the acceptor states. This implies that the stress can change both the energy and the oscillator strength of a radiative transition between levels. An absorption line may be switched from strong to weak or conversely by applying stress.

### 3.3. Extra degeneracy

It is worth mentioning that the decoupling between HH and LH in the high-stress region can cause extra degeneracy, as can be seen from figures 1(b) and 2(b). In this extreme situation, the effective-mass Hamiltonian has nearly azimuthal symmetry and the acceptor states can be regarded as belonging to a single valence band. As a result, the wavefunctions of the acceptor states can be expressed as

$$\Psi_{JM}^u = \sum_{l \geq |m|}^{(u)} f_{JM}^{lm}(r) Y_{lm}(\theta, \phi) \Phi_M^J \quad (8)$$

with  $J$ ,  $M$ ,  $m$  and  $u$  as good quantum numbers, where  $u$  is the parity of the envelope function. The sum in equation (8)

**Table 4.** Combinations of two-dimensional representations for extra degeneracy, if possible, in the limiting case of high stress. They depend on the Bloch function, the magnetic quantum number  $m$  and the parity. The  $n$  is a positive integer. Only combinations of the even-parity representations are listed. For combinations of the odd-parity representations, just change  $\Gamma_6^+$  and  $\Gamma_7^+$  to  $\Gamma_6^-$  and  $\Gamma_7^-$ , respectively.

$\Phi_M^{(J)}$	$ m $	Combinations
$\Phi_{\pm 3/2}^{(3/2)}$	0	$\Gamma_6^+$
	$2n - 1$	$\Gamma_6^+ + \Gamma_7^+$
	$4n$	$2 \times \Gamma_6^+$
	$4n - 2$	$2 \times \Gamma_7^+$
$\Phi_{\pm 1/2}^{(3/2)}$	0	$\Gamma_7^+$
	$2n - 1$	$\Gamma_6^+ + \Gamma_7^+$
	$4n$	$2 \times \Gamma_7^+$
	$4n - 2$	$2 \times \Gamma_6^+$

runs over even  $l$  for  $u = +1$  (or simply  $+$ ) and over odd  $l$  for  $u = -1$  (or simply  $-$ ). The azimuthal and the time-reversal symmetries ensure the fourfold degeneracy in the states  $\Psi_{JMm}^u$ ,  $\Psi_{J,M,-m}^u$ ,  $\Psi_{J,-M,m}^u$  and  $\Psi_{J,-M,-m}^u$  for  $m \neq 0$  and the twofold degeneracy in the states  $\Psi_{JM0}^u$  and  $\Psi_{J,-M,0}^u$  for  $m = 0$ . Because the  $\Gamma_6^u$  and the  $\Gamma_7^u$  representations are both doubly degenerate, there are three possible combinations in the high-stress case for the extra degeneracy,  $\Gamma_6^u + \Gamma_7^u$ ,  $2 \times \Gamma_6^u$  and  $2 \times \Gamma_7^u$ , for  $m \neq 0$ , and no extra degeneracy for  $m = 0$ . The combinations depend on the values of  $m$ ,  $u$  and  $M$ , as listed in table 4. In the table, we list the combinations only for even-parity states. For combinations of odd-parity states, simply change  $\Gamma_6^+$  and  $\Gamma_7^+$  to  $\Gamma_6^-$  and  $\Gamma_7^-$ , respectively. For HH-like states ( $M = \pm 3/2$ ), the representations without extra degeneracy are  $\Gamma_6^+$  and  $\Gamma_7^+$  for  $m = 0$ , and the combinations with extra degeneracy include (i)  $\Gamma_6^{\pm} + \Gamma_7^{\pm}$  for  $|m| = 2n - 1$ , (ii)  $2 \times \Gamma_6^{\pm}$  and  $2 \times \Gamma_7^{\pm}$  for  $|m| = 4n$ , and (iii)  $2 \times \Gamma_6^{\pm}$  and  $2 \times \Gamma_7^{\pm}$  for  $|m| = 4n - 2$ , where  $n$  is a positive integer. For LH-like states ( $M = \pm 1/2$ ), the possible degeneracies can be obtained from those for the HH-like states just by interchanging the parities  $+$  and  $-$ . The results for the LH-like states are also listed in table 4. We emphasize that only the  $\Gamma_7^+$  and the  $\Gamma_6^-$  states (the  $\Gamma_6^+$  and the  $\Gamma_7^-$  states) can remain doubly degenerate without extra degeneracy at high compressive (tensile) stress, in agreement with the results in figures 1 and 2.

### 3.4. Chemical shifts

We have just discussed the stress dependence of the energy levels of the isocoric acceptor Ga in Ge and have also presented the energy levels of even-parity states for the nonisocoric group III acceptors in strainless Ge. Now we are going to explore the stress effect on the energy levels of even-parity states for various nonisocoric group III acceptors in Ge. Figure 5 shows the chemical shifts of several low-energy even-parity states versus [001] stress for nonisocoric acceptors B, Al, In and Tl, as well as the isocoric acceptor Ga, doped in Ge. The chemical shift of a state for a certain species of acceptor is defined as the deviation of the energy level of the state from the corresponding level which is obtained by setting the central-cell correction  $V_{cc}$  at zero (i.e.  $A = 0$ ). It is caused by the

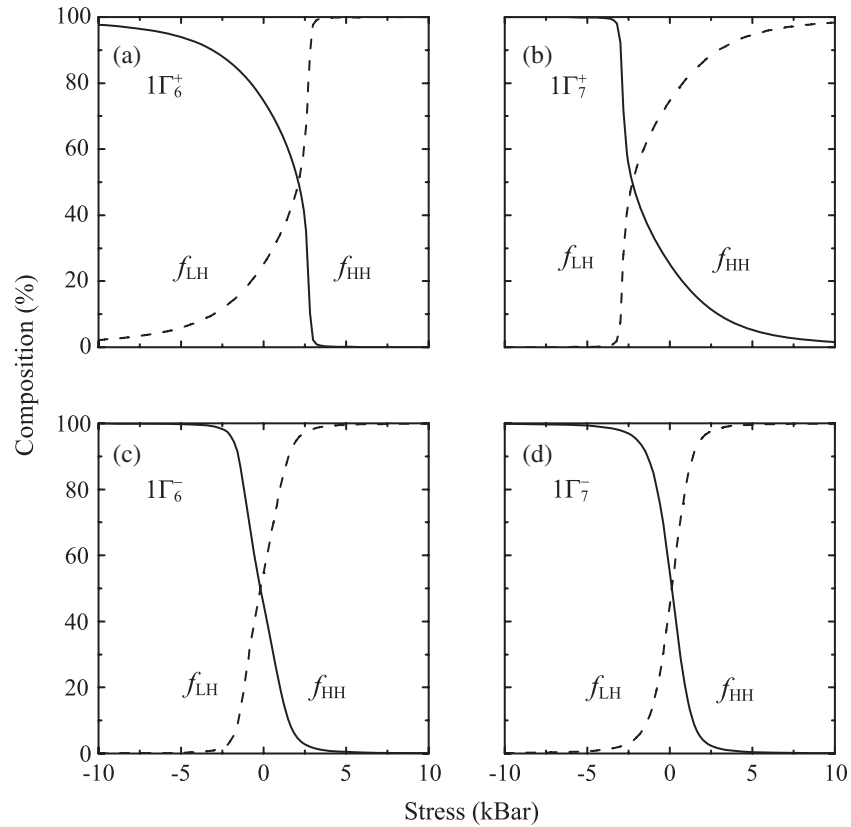


**Figure 4.** Stress dependence of the HH composition ( $f_{HH}$ ) and the LH composition ( $f_{LH}$ ) of (a)  $1\Gamma_6^+$ , (b)  $1\Gamma_7^+$ , (c)  $1\Gamma_6^-$  and (d)  $1\Gamma_7^-$  for Ge:Ga. The positive (negative) stress means a compressive (tensile) stress.

central-cell correction which has been included in equation (4). Due to the short-range nature of the central-cell potential, the chemical shift can be considered to be nearly proportional to the value of  $A$  times the probability density of the hole at the acceptor site. Since only the  $s$  ( $l = 0$ ) component of the wavefunction contributes probability at the acceptor site, the chemical shift should be proportional approximately to  $A \sum_{v=1}^6 |f_v^{00}(0)|^2$ . As a result, the chemical shifts for Ga are negligibly small, as can be seen from figure 5, because of the small value of  $A$ . Also, the chemical shifts for B and Al are positive and those for In and Tl are negative in accordance with the signs of their  $A$  values, which reflects a positive or negative change in the effective force on the hole exerted by the core states. However, the chemical shift does not linearly depend on  $A$ . A negative  $A$  enhances the total attractive force of the acceptor acting on the hole and causes the wavefunctions to be more localized around the acceptor site than a positive  $A$ . As a result, the chemical shift for Tl is more predominant than for B although the  $A$  value for Tl is smaller in magnitude. For In, the chemical shift can be comparable to that for B although the magnitude of  $A$  is only about one-half of that for B.

We know from table 4 the asymptotic property that the  $\Gamma_6^+$  ( $\Gamma_7^+$ ) states have no significant  $m = 0$  component at high compressive (tensile) stress. This implies that the  $s$  components of the  $\Gamma_6^+$  ( $\Gamma_7^+$ ) states decrease to zero with the compressive (tensile) stress. This can explain the asymmetric stress dependence of the chemical shift in figure 5 wherein the magnitude of the chemical shift for the  $\Gamma_6^+$  ( $\Gamma_7^+$ ) states

decreases to almost zero with the compressive (tensile) stress much more rapidly than with the tensile (compressive) stress. On the other hand, the relatively mild stress dependence for the  $\Gamma_6^-$  ( $\Gamma_7^-$ ) states in the high tensile (compressive) stress region is caused by the distortion of the wavefunctions whose  $s$  components reduce with the deformation.

### 3.5. Line assignment for acceptors in Ge under stress

Dickey and Dimmock [17] have measured absorption spectra for acceptors Ga, In and Tl in Ge under uniaxial stress along [001] using polarized radiation and have assigned the  $B$ ,  $C$  and  $D$  absorption lines with group-theoretical consideration. They mis-regarded the final state of the  $B$  line transition as a  $\Gamma_7^-$  state at zero stress. This led to an incorrect conclusion that the  $1\Gamma_8^+$  state split into the  $1\Gamma_6^+$  and the  $1\Gamma_7^+$  states under [001] stress with the  $1\Gamma_6^+$  states as the ground state. The error in the order between the  $1\Gamma_6^+$  and the  $1\Gamma_7^+$  levels further resulted in some inappropriate assignments of the  $C$  and  $D$  line components. Although later theoretical works have correctly identified the  $1\Gamma_7^+$  state as the ground state under [001] stress [16], reassignment for the transition lines is still incomplete. Vickers *et al* [18] have resolved the ten  $C$  line components and the four  $D$  line components by experiment and also made an appropriate assignment. However, the  $B$  line components have not been correctly assigned till now. To complete the identification of the  $B$  line components, we first note that the final state of the  $B$  line in the absence of stress



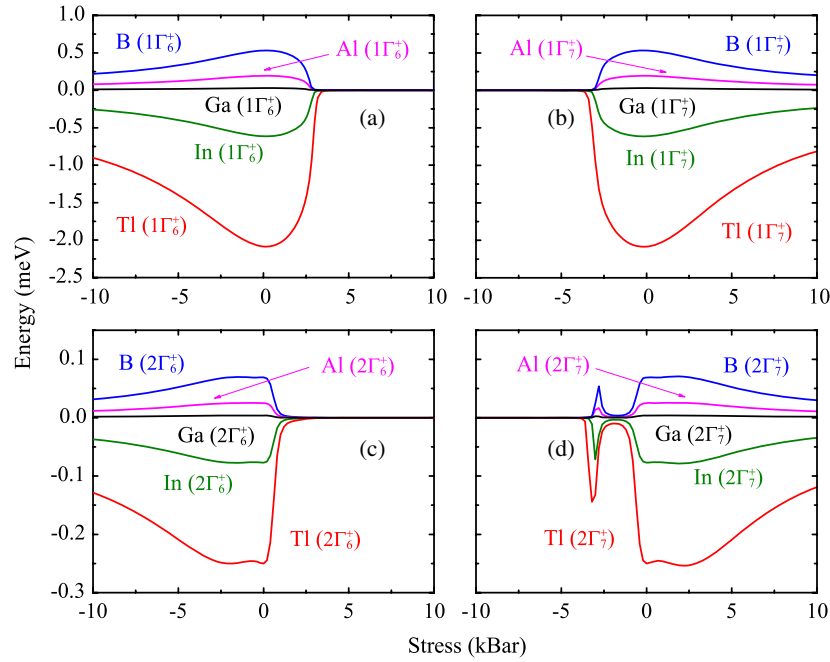


**Figure 5.** Chemical shifts of (a)  $1\Gamma_6^+$ , (b)  $1\Gamma_7^+$ , (c)  $2\Gamma_6^+$  and (d)  $2\Gamma_7^+$  as functions of [001] stress for various group III acceptors in Ge. The positive (negative) stress means a compressive (tensile) stress.

should be the  $4\Gamma_8^-$  state instead of a  $\Gamma_7^-$  state, as can be seen from table 3. It follows that, in the presence of [001] stress, the  $B$  line splits into four components,  $B_1$  ( $1\Gamma_6^+ \rightarrow 4\Gamma_6^-$ ),  $B_2$  ( $1\Gamma_6^+ \rightarrow 5\Gamma_7^-$ ),  $B_3$  ( $1\Gamma_7^+ \rightarrow 4\Gamma_6^-$ ) and  $B_4$  ( $1\Gamma_7^+ \rightarrow 5\Gamma_7^-$ ), because the  $4\Gamma_8^-$  state splits into the  $4\Gamma_6^-$  and the  $5\Gamma_7^-$  states. According to our calculation of oscillator strengths [28], we predict that the  $B_1$  and the  $B_4$  transitions are more difficult to observe than the  $B_2$  and the  $B_3$  transitions. This is in agreement with the fact that only the  $B_2$  and the  $B_3$  transitions have been observed till now by experiment. Figure 6 shows the newly assigned transition energies of the  $B$ ,  $C$  and  $D$  line components for Ge:In against the [001] stress, together with the experimental data of Dickey and Dimmock [17] for comparison. The excellent agreement with the experimental data confirms the reliability of our calculation in the low-stress region.

Figure 7 shows a comparison between our calculation and the experimental result of Vickers *et al* [18] on the stress dependence of the  $C^*$  and the  $D^*$  related levels for Ge:Ga, where, as defined by Gershenson *et al* [19], the  $D^*$  corresponds to the  $2\Gamma_8^-$  level which splits into  $2\Gamma_6^-$  and  $2\Gamma_7^-$  under [001] stress. To comply with the data of Vickers, our calculated energy levels are measured from a stress-dependent energy reference  $E(1\Gamma_8^+) - P_\epsilon$ , where  $E(1\Gamma_8^+)$  is the energy level of the ground state  $1\Gamma_8^+$  at zero stress and  $P_\epsilon$  is the strained energy induced by hydrostatic compression. The agreement is fairly good except on the relative position between the  $3\Gamma_6^+$  and the  $3\Gamma_7^+$  levels. There is no artificial energy shift in our calculation for the data in figure 7.

### 3.6. Justification for the model potential

Finally, it is worth discussing the validity of our calculation based on the effective-mass theory with the semi-empirical

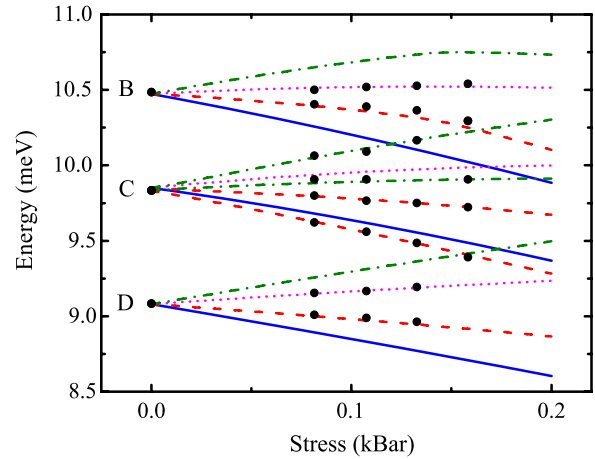


**Figure 6.** Stress dependence of transition energies of the  $B$ ,  $C$  and  $D$  lines for Ge:In. The solid circles represent the experimental data taken from [17]. The lines are for the calculated transition energies from the  $1\Gamma_6^+$  to the  $\Gamma_6^-$  states (solid lines), from the  $1\Gamma_6^+$  to the  $\Gamma_7^-$  states (dashed lines), from the  $1\Gamma_7^+$  to the  $\Gamma_6^-$  states (dotted lines) and from the  $1\Gamma_7^+$  to the  $\Gamma_7^-$  states (dash-dotted lines).

potential. Such a calculation scheme, as we have seen, has yielded an excellent agreement with experiment for stress up to 0.35 kbar. However, we have shown and analyzed our calculated results for stress up to 10 kbar. We do not find high-stress experimental data in the literature to confirm the validity of our calculation. In fact, the so-called high stress of 10 kbar gives the normal strain  $\epsilon_z$  along the uniaxial axis as small as  $-0.97\%$  for Ge. Under small stress, the Bir-Pikus effective-mass theory [20] is still applicable and other stress effects should give a negligible higher-order correction. For instance, we have supposed the functional form of the

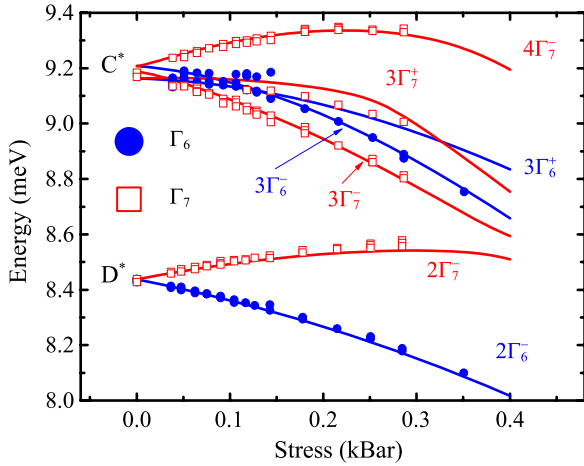


**Figure 7.** Stress dependence of the  $C^*$  and the  $D^*$  line components for Ge:Ga. The energies are measured from a stress-dependent reference  $E(1\Gamma_8^+) - P_\epsilon$ , where  $E(1\Gamma_8^+)$  is the energy level of the ground state  $1\Gamma_8^+$  at zero stress and  $P_\epsilon$  is the strained energy induced by hydrostatic compression. The solid lines are the results of the present work. The solid circles (open squares) denote the experimental data associated with the  $\Gamma_6$  ( $\Gamma_7$ ) final states taken from [18].

semi-empirical impurity potential  $V$  introduced in equation (4) to be independent of the stress in the calculation. To justify the assumption, we reconsider the impurity potential as contributed from two parts [6]. One is called the bare potential  $V_b$ , which is caused by the difference in the charges of the closed-shell ions (namely, the nuclei plus the core electrons) between the crystals with and without the impurity present. The other one is caused by the redistribution of valence electrons due to the presence of the impurity and is called the screening potential  $V_s$  since, from the viewpoint of the hole of interest, the valence electrons play a role in screening the bare potential. It is reasonable to assume the inner states of all the closed-shell ions to be unaffected by the presence of the impurity, except for the state of the host ion to be replaced by the impurity ion. As a result, the presence of the impurity gives a bare potential as the Coulomb potential due to a point charge at the impurity site. Furthermore, the stress as small as we have considered should not alter significantly the inner states of the host and the impurity ions. Neglecting the lattice relaxation due to the presence of the impurity, we conclude that the strain causes a change only in the screening potential, in addition to the deformation of the lattice which has been considered by the Bir–Pikus theory.

The  $q$ -dependent dielectric screening of the impurity potential in equation (4) is based on the assumptions that the distribution of valence electrons responds linearly to the presence of the impurity and that the Umklapp elements of the dielectric tensor are neglected [11]. According to our previous argument, the assumptions should be valid regardless of the applied stress we have considered. In other words, the functional form of the impurity is applicable not only for low stress ( $<0.35$  kbar), as has been confirmed by the observed transition energies, but also for stress up to 10 kbar if we allow the dielectric constant  $\epsilon$  to be a function of the stress.

As has been pointed out, the correction due to the stress dependence of  $\epsilon$  should be small compared to the Bir–Pikus strain effect. Goi *et al* [29] have measured the stress dependence of  $\epsilon$  for Ge at room temperature, giving

$$\epsilon(P, T = 300 \text{ K}) = 15.94 - 0.36P + 0.014P^2, \quad (9)$$

where  $P$  is the hydrostatic stress (in units of 10 kbar). To obtain an expression for low temperature, we suppose the variation of temperature also gives a small effect on  $\epsilon$  such that  $\epsilon$  can be expressed as a separable function of  $P$  and  $T$ , namely a function in a product of functions only of  $P$  and only of  $T$ . Accordingly, the dielectric constant at  $T = 0$  K is

$$\begin{aligned} \epsilon(P, T = 0 \text{ K}) &= \epsilon(0, 0 \text{ K})\epsilon(P, 300 \text{ K})/\epsilon(0, 300 \text{ K}) \\ &= 15.36 - 0.347P + 0.0135P^2, \end{aligned} \quad (10)$$

where we have used  $\epsilon(0, 0 \text{ K}) = 15.36$  [26]. As expected, we see that the stress dependence of  $\epsilon$  is small for the stress up to 10 kbar. For the uniaxial stress  $\sigma$  along the [001] direction in our case, the stress dependence of  $\epsilon$  can be obtained from equation (10) by replacing the coefficient in the linear-in- $P$  term with its one-third and neglecting the last term. This results in  $\epsilon(\sigma) = 15.36 - 0.116\sigma$ . It gives a correction of no more than 2.2% for the energy levels and a correction of no more than 4.6% for the chemical shifts for a stress of 10 kbar.

## 4. Conclusions

We have calculated and analyzed the electronic structures of various group III acceptors in Ge under [001] stress based on the effective-mass theory with a semi-empirical impurity potential. We have identified systematically the even-parity states by newly assigning the transition lines. In addition, our calculation has resolved crowding levels of final states for observed single transition lines. The stress effect on the binding energies of acceptor states has been found to be related to the compositions of the states. Our results show that the binding energies decrease rapidly with the stress in the low-stress region ( $<3$  kbar). Also, the binding energies of even-parity states exhibit remarkable asymmetry in the stress dependence due to the large difference between the HH and the LH compositions of the states. They decrease much more rapidly with compressive stress than with tensile stress for  $\Gamma_6^+$  states, but conversely for  $\Gamma_7^+$  states. Increasing stress can cause HH–LH decoupling. The acceptor states asymptotically approach pure HH (LH) states with the compressive (tensile) stress. In the limiting case of high stress, extra degeneracy occurs among the states with nonzero magnetic quantum numbers. The central-cell correction is important for energy levels of nonisocoric acceptors and causes significant chemical shift for even-parity states, especially for the  $1\Gamma_6^+$  and the  $1\Gamma_7^+$  states. The compressive (tensile) stress can reduce effectively the chemical shift of the  $\Gamma_6^+$  ( $\Gamma_7^+$ ) states because of the rapid reduction of the  $s$  component with the stress. We have completed the assignment of the four line components into which the  $B$  line splits under stress. Our calculation has given an excellent agreement with experiment for stress up to 0.35 kbar. A detailed argument has been made supporting the applicability of our calculation scheme to the case of high stress.

## Acknowledgment

This work was supported by the National Science Council of the Republic of China under contract no. 97-2221-E-009-164-.

## References

- [1] Jones R L and Fisher P 1965 *J. Phys. Chem. Solids* **26** 1125
- [2] Soepangkat H P and Fisher P 1973 *Phys. Rev. B* **8** 870
- [3] Haller E E and Hansen W L 1974 *Solid State Commun.* **15** 687
- [4] Skolnick M S, Eaves L, Stradling R A, Portal J C and Askenazy S 1974 *Solid State Commun.* **15** 1403
- [5] Luttinger J M 1956 *Phys. Rev.* **102** 1030
- [6] Pantelides S T and Sah C T 1974 *Phys. Rev. B* **10** 621
- [7] Pantelides S T and Sah C T 1974 *Phys. Rev. B* **10** 638
- [8] Austin B J, Heine V and Sham L J 1962 *Phys. Rev.* **127** 276
- [9] Baldereschi A and Lipari N O 1976 *Proc. 13th Int. Conf. Phys. Semicond.* ed F G Fumi (Rome: Tipografia Marves) p 595
- [10] Lipari N O and Baldereschi A 1978 *Solid State Commun.* **25** 665
- [11] Lipari N O, Baldereschi A and Thewalt M L W 1980 *Solid State Commun.* **33** 277
- [12] Buczko R and Bassani F 1992 *Phys. Rev. B* **45** 5838
- [13] Aleshkin V, Gavrilenko L, Odnoblyudov M and Yassievich I 2008 *Semiconductors* **42** 880 and references therein
- [14] Broeckx J, Clauws P and Vennik J 1986 *J. Phys. C: Solid State Phys.* **19** 511
- [15] Broeckx J and Vennik J 1987 *Phys. Rev. B* **35** 6165
- [16] Buczko R 1987 *Nuovo Cimento D* **9** 669
- [17] Dickey D H and Dimmock J O 1967 *J. Phys. Chem. Solids* **28** 529
- [18] Vickers R E M, Fisher P and Freeth C A 1988 *Solid State Commun.* **65** 271
- [19] Gershenzon E M, Gol'tsman G N and Kagane M L 1977 *Sov. Phys.—JEPT* **45** 769
- [20] Bir G L and Pikus G E 1974 *Symmetry and Strain Induced Effects in Semiconductors* (New York: Wiley)
- [21] Chao C Y P and Chuang S L 1992 *Phys. Rev. B* **46** 4110
- [22] Binggeli N and Baldereschi A 1988 *Solid State Commun.* **66** 323
- [23] Hensel J C and Suzuki K 1974 *Phys. Rev. B* **9** 4219
- [24] Aggarwal R L 1970 *Phys. Rev. B* **2** 446
- [25] Madelung O 2004 *Semiconductors: Data Handbook* (Berlin: Springer)
- [26] Faulkner R A 1969 *Phys. Rev.* **184** 713
- [27] Kurskii Y A 1993 *Phys. Rev. B* **48** 5148
- [28] Wang T H and Yen S T 2009 unpublished
- [29] Goi A R, Syassen K and Cardona M 1990 *Phys. Rev. B* **41** 10104